Statistics of Numerical Experiments with Multi-Fracture Systems

E. Holzbecher[1]
[1.] Department of Applied Geosciences, German University of Technology in Oman (GUtech), Muscat, Oman

Introduction

Modeling of fractured porous media systems is currently of high interest in various academic and applied fields, mainly in geological and material sciences. There are various modeling approaches for fracture systems, as outlined recently by Berre *et al.* (2019). In multi-continuum models the details of the fracture systems are not considered. In contrast discrete fracture networks (DFN) are capable of representing the fractures and their connections accurately, but neglect the background medium. Discrete-fracture matrix models (DFM) thus form a compromise, in which both background medium and fractures are considered with equal accuracy.

The very different scales of the region of an application case on the larger part and the fracture on the lower part pose a challenge for modeling. Computational resources may be exceeded if the fracture flow is modeled in detail on the small scale. Thus a mixed dimensional approach is often given preference (Schwenck *et al.* 2015). Representing the fractures in a lower dimension than the entire region (i.e. 1D in 2D, and 1D or 2D in 3D) enables the modeling of multi-fracture systems with a multitude of fracture objects.

For 1D fractures in 2D analytical solutions can be formulated (Sato 2015, Nadlal & Weijermars 2019). However, for a model with a large number of fractures modeling becomes tedious. Numerical methods become more flexible and easy to use.

For a single fracture Romano-Perez & Diaz-Viera (2015) compared various conceptual approaches and found DFM 'using the embedded fracture approach ... much more simple and flexible to implement in comparison'. For a fracture as a thin structure Holzbecher (2020) compared several approaches and found fitting results from numerical and analytical methods that are based on the hydraulic head formulation (see below). In both studies COMSOL Multiphysics was used for numerical modeling. Kristinof *et al*. (2010) used COMSOL to simulate air and water flow through a specimen of granite with a single vertical fracture, finding 'a good satisfactory agreement' of model and experimental results.

Here we use the software to deal with multiple fractures. In a study on a network of cracks Perko *et al*. (2011) conclude: 'we have thus demonstrated that implementing cracks in COMSOL for flow and transport simulations produces adequate results and is fit for purpose for use in the analysis of saturated fractured porous media'.

Methods

Within the Subsurface Module of COMSOL Multiphysics the option for mixed-dimensional modeling is available as a sub-mode of models, based on Darcy's Law. Darcy's Law mode solves the differential equation for pressure p:

$$\nabla \frac{k}{\mu} \nabla \left(p + \rho g z \right) = Q_m \tag{1}$$

with Darcy velocity Q_m, permeability k, fluid dynamic viscosity μ and density ρ. g denotes the acceleration due to gravity and z is the space coordinate in direction opposite to gravity. Equation (1) holds generally for stationary laminar flow in porous media in 1D, 2D or 3D, if the Reynolds number is lower than 10. In its 1D formulation it can be used for fracture flow in a 2D porous matrix or for channel flow in a 3D porous matrix. The 2D formulation can be applied for fractures in 3D domains.

In our experiments we deal with 1D fractures in a 2D porous domain. Moreover we neglect density effects. If there are no additional sinks or sources, the equation can be simplified to:

$$\nabla K \nabla h = 0 \tag{2}$$

where hydraulic conductivity K and piezometric head h are related to pressure and permeability by:

$$K = \frac{k \rho g}{\mu} \quad \text{and} \quad h = \frac{p}{\rho g} \tag{3}$$

We examine the characteristics of multi-fracture systems in 2D, where fractures are treated as 1D line segments. A multitude of scenarios with a randomly generated fracture network is created using the option to define user-defined method.

```
model.methodCall("methodcall5").run();
while (ind < NUMBER_OF_FRACTURES) {
  hx = Math.random()*MODEL_LENGTH;
  hy = Math.random()*MODEL_LENGTH;
  ha = Math.random()*Math.PI;
  hl = Math.pow(lmax, alfa)-(Math.pow(lmax, alfa)-Math.pow(lmin, alfa))*Math.random();
  hl = Math.pow(hl, 1/alfa);
  model.component("comp1").geom("geom1").create("ls1"+ind, "LineSegment");
  with(model.component("comp1").geom("geom1").feature("ls1"+ind));
    set("specify1", "coord");
    set("coord1", new double[]{hx+0.5*hl*Math.cos(ha), hy+0.5*hl*Math.sin(ha)});
    set("specify2", "coord");
    set("coord2", new double[]{hx-0.5*hl*Math.cos(ha), hy-0.5*hl*Math.sin(ha)});
  endwith();
  model.component("comp1").geom("geom1").feature("ls1"+ind).set("contributeto", "mf1");
  ind++;
}
```

Figure 1. Snippet of method coding

Figure 1 shows a snippet of the main part of the method code. Input parameters are the number of fractures, the minimum and maximum fracture length and the power of the

probability distribution for the fracture length. Within each run in the while-loop a fracture is created.

Figure 2 shows an example set-up with 20 fractures and the FE mesh for the numerical calculations. Here we chose uniform probability for a fracture length between a minimum of 0.01 and a maximum of 0.7. These length units are dimensionless, normalized to the side length of the system. The FE mesh is depicted also.

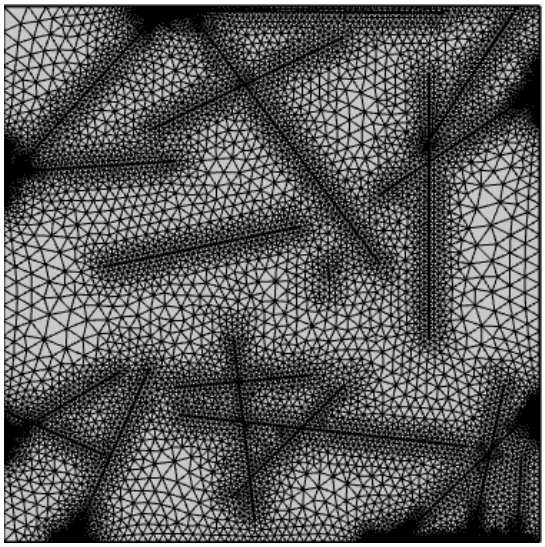

Figure 2. Example set-up with 20 fractures and finite element mesh

In the model a hydraulic gradient Δh is applied, in the depicted figures in horizontal direction, from left to right. Upper and lower boundaries are of no-flow type.

As post-processing for each scenario the effective hydraulic conductivity as major hydraulic property of the entire system is determined. It is computed from the total normal flux at the inflow or outflow boundary by line integration:

$$K_{eff} = \frac{\int u_x \, dy}{\Delta h} \qquad (4)$$

Evaluating the integral on the left (inlet) or right (outlet) lead to marginal differences for the cases that are reported here. This check of accuracy failed for systems with long fractures and high conductivity ratios.

Input parameters for a reference case scenario are shown in Table 1. We examine the influence of the following multi-fracture characteristics: number of fractures, minimum and maximum fracture length, fracture thickness, grid refinement, fracture and matrix conductivity as well as the ratio between fracture and matrix conductivities.

In order to examine the influence of the fracture network characteristic values of the reference setting are altered to obtain new constellations. For each of the constellations a set of 40 scenarios is run, and for each scenario the effective hydraulic conductivity is evaluated according to formula (4).

Table 1: Parameter values of the reference case

Parameter	**Value [Unit]**
Domain length	1 [m]
Domain width	1 [m]
Fracture conductivity $K_{fracture}$	0.01 [m/s]
Matrix conductivity K_{matrix}	10^{-6} [m/s]
Head gradient	1 [-]
Fracture aperture	5 [mm]
Minimum fracture length	1 [mm]
Maximum fracture length	0.3 [m]
Number of fractures	40

Results

Figure 3 illustrates the flow field in two out of a multitude of scenarios. The colormap shows hydraulic head, decreasing from the inflow boundary on the left to the outlet on the right. Fractures are depicted by black lines. Grey lines represent streamlines.

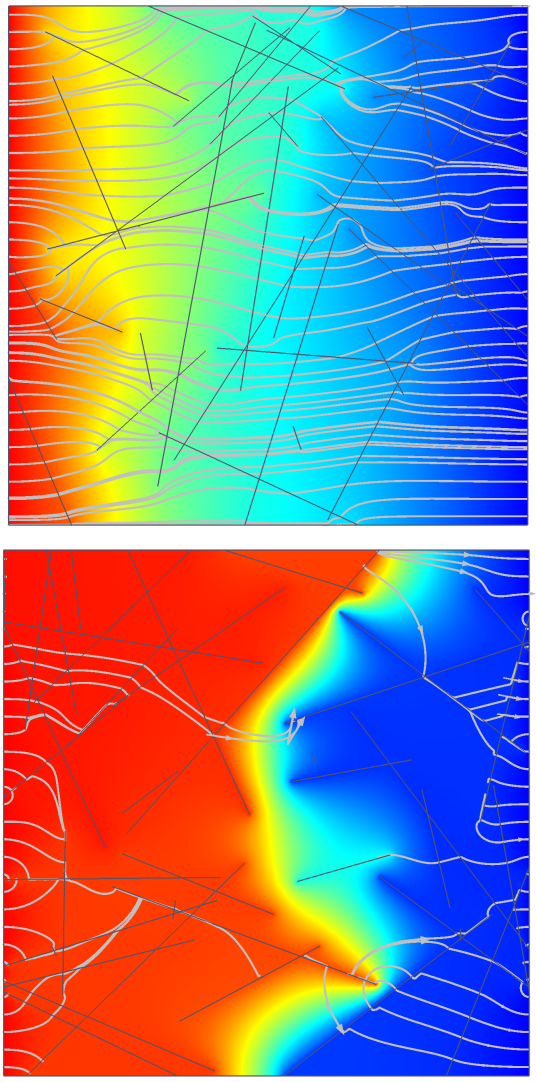

Figure 3. Flow pattern examples for two scenarios, showing fractures (black), colormap of piezometric head and streamlines (light grey)

The upper figure shows a result for a scenario in which the conductivity in the fractures is 100 higher than the conductivity in the matrix. The lower figure was obtained for a scenario with a high conductivity ratio $K_{fracture}/K_{matrix}$ of 10000. In the latter case the local gradients within the system are obviously higher. Furthermore the gradient halfway through the system, where there are no connected fractures, is particularly high.

In Figures 3 one can clearly observe an increase of the streamline density near to the ends of fractures with dominating horizontal orientation. There is a reduced hydraulic gradient along these fractures. This effect is stronger for the scenario with higher conductivity contrast between fracture and matrix. It can be noted that not all streamlines can be traced through the entire system. Several streamlines get stuck within the fractures, a numerical effect that could not completely avoided even with refined meshes and altered tracing options.

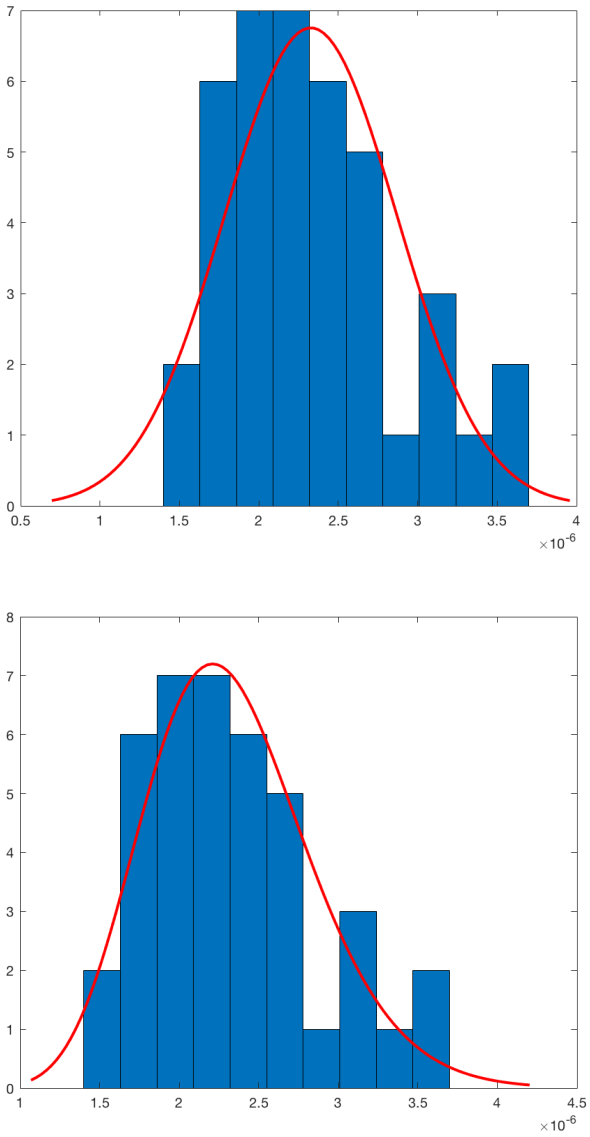

Figure 4. Example of the hydraulic conductivity distribution from 40 scenario runs with fitted statistics; top: fitted normal distribution, bottom: fitted to gamma distribution

As an example for the variation of hydraulic conductivity Figure 4 depicts results for reference case parameters except for the maximum fracture length of 0.6. Conductivity ratios range from 1.5 up to 3.6 10^{-6} m/s. The mean value is 2.3 10^{-6} m/s and the variance 5.4 10^{-7} m/s. In red color the figures show the fitted normal distribution (top) and the gamma distribution. Here the fracture systems lead to an increase of conductivity by a factor of 2.3 in average. In the sequel we will report the relative conductivities only.

From the reference system, given by the parameter values in Table 1, we ran scenario sets with the value of a single parameter changed. We chose three or four different values for each parameter. In the following we report the detail results for some of these parameter variations.

The statistics of the values for the scenarios are shown in the following boxplots. On the ordinate we show the increase of conductivity as effect of preferential flow through the fracture system, i.e. the effective conductivity in relation to the matrix conductivity K_{eff}/K_{matrix}.

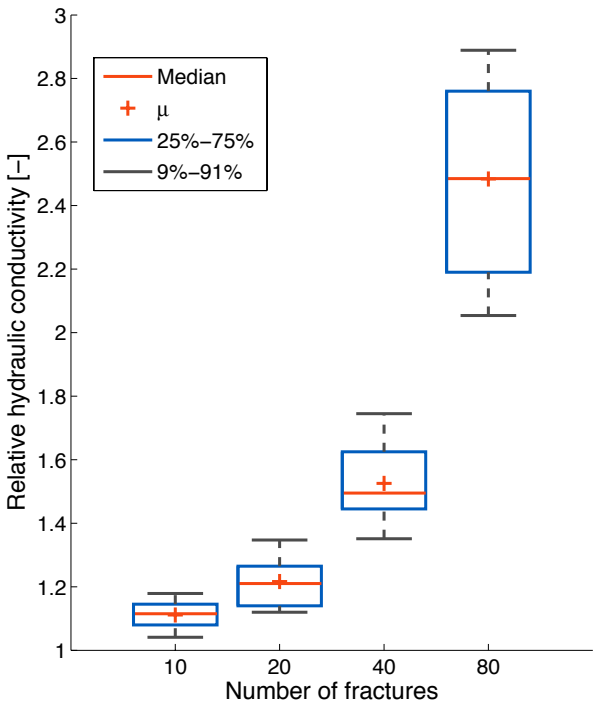

Figure 5. Boxplot showing mean, median and percentiles of relative hydraulic conductivity in dependency of the number of fractures within the model domain

The number of fractures was varied, constructing 10, 20, 40 or 80 fractures within the unit domain. Figure 5 shows the increase of effective hydraulic conductivity of the fractured system. For each of the four constellations the box plot depicts median, mean (μ), as well as 25%-75% and 9%-91% percentiles. For the smallest number of fractures (10) the conductivity can be expected to increase by approximately 10% only, while it increases by a factor of roughly 2.5 (in the mean), if there are 80 fractures present in the domain. As expected the relative conductivity increases with the number

of fractures, taking the values of 1.11, 1.22, 1.53 and 2.48 for the four constellations. Also the standard deviation is increasing with the values 0.047, 0.097, 0.15 and 0.35. Using the K_{eff} values for curve fitting leads to a linear relationship (R^2=0.9756), in which each additional fracture in the mean leads to a relative increase of conductivity of 0.02.

The maximum fracture length was changed taking the values 0.15, 0.3, 0.45 and 0.6 in the unit domain. The statistics of the outcomes of the model runs is presented in the boxplots of Figure 6. Here also a clear trend is observed. The mean values of conductivity are 1.05, 1.22, 1.61 and 2.33. The standard deviations are 0.013, 0.097, 0.22 and 0.54. Curve fitting with these values leads to a good quadratic relationship (R^2=0.9917)

$$K_{eff} / K_{matrix} = 1.53 - 4.05x + 9.33x^2 \quad (5)$$

and an optimal cubic relationship (R^2=1):

$$K_{eff} / K_{matrix} = 0.76 + 4.11x - 15.11x^2 + 21.73x^3 \quad (6)$$

where x denotes the maximum fracture length.

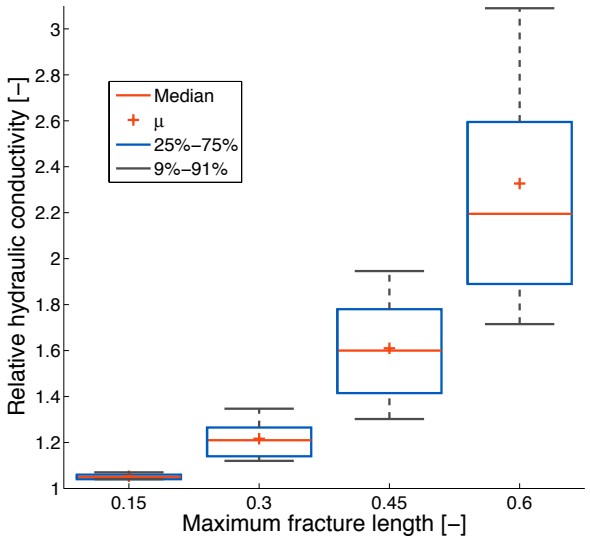

Figure 6. Boxplot showing mean, median and percentiles of relative hydraulic conductivity in dependency of the maximum fracture length

In the same manner we also examined the influence of the minimum fracture length (values: 0.01, 0.02, 0.05 and 0.1) and fracture thickness were examined. In both cases no pronounced dependency could be recognized. For the minimum fracture length there was a slight negative correlation, as the means of the relative effective conductivity decreased from 1.22 to 1.1 with increasing minimum length. Independent of the chosen fracture thickness we obtained a mean increase of the effective hydraulic conductivity by 22% independent of the fracture aperture.

For an examination of the conductivity ratio $K_{fracture}/K_{matrix}$ we used the values 100, 1000 and 10000. The results are shown in the boxplots of Figure 7. The mean values obtained are 1.05, 1.17 and 1.23, with standard deviations 0.15, 0.46 and 0.59.

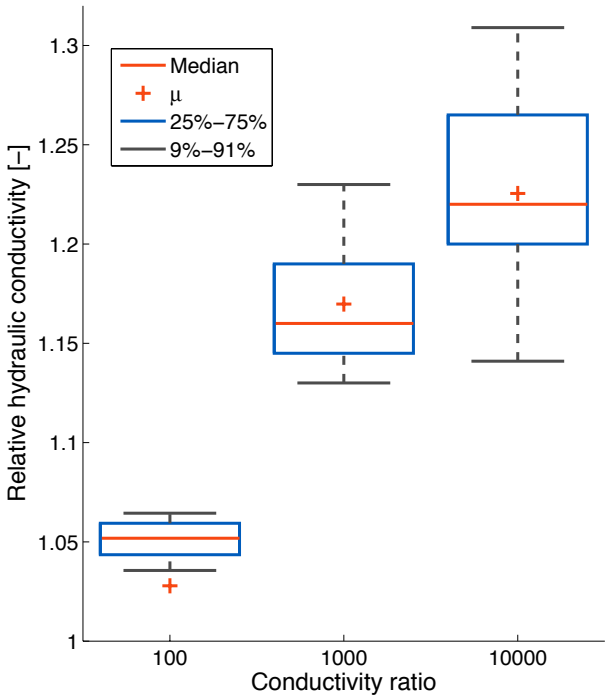

Figure 7. Boxplot showing mean, median and percentiles of relative hydraulic conductivity in dependency of the conductivity ratio

The dependency on the conductivity ratio was also studied for fracture lengths following a power law distribution. In the implementation it is utilized that a uniformly distributed variable *y* can be transformed into a power law distribution x with negative exponent α by using the formula (Radicchi 2014):

$$x = x_{\max}^{\alpha+1} - (x_{\max}^{\alpha+1} - x_{\min}^{\alpha+1}) y^{1/(\alpha+1)} \quad (7)$$

where $x_{\min}$ and $x_{\max}$ denote the interval boundaries. Its implementation in a COMSOL method is shown in the code snipped in Figure 1. The parameters for these simulations are given in Table 2.

Table 2: Fracture lengths power law parameters

Parameter	Value [Unit]
Minimum fracture length $x_{\min}$	1 [cm]
Maximum fracture length $x_{\max}$	0.9 [m]
Exponent α	-1.7

As described before simulations were run for fracture conductivities being 10, 100, 1000 and 10000 times higher than matrix conductivity. We obtained factors of 1.08, 1.13, 1.155 and 1.162 for mean conductivity increase from background. The standard deviations for these runs were: 0.024, 0.13, 0.3 and 0.37. Boxplot visualizations for these results are depicted in Figure 8.

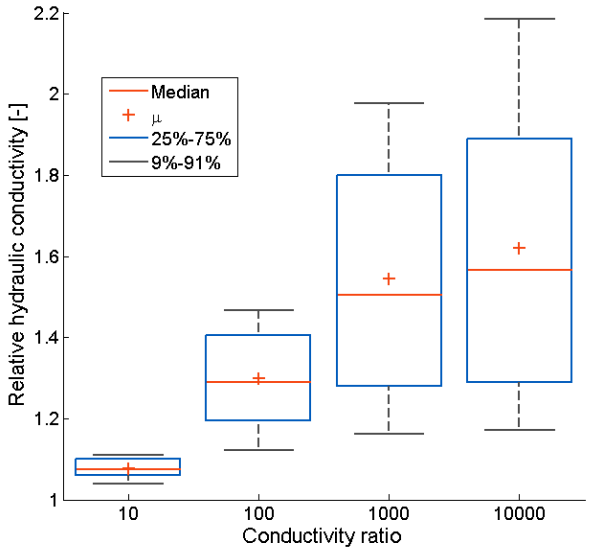

Figure 8. Boxplot showing mean, median and percentiles of relative hydraulic conductivity in dependency of the conductivity ratio

Conclusions

A multi-fracture model has been set up for the evaluation of effective hydraulic conductivity as affected by the characteristics of the fracture network. The model is non-dimensionalized, in order to obtain results independent of the actual spatial extension of the region, the head gradient and the hydraulic conductivity of the matrix. There is also no dependency on the porosities in the fractures and the background material.

Multiple sets of scenarios have been run in 2D with randomly determined fractures, modeled as line segments of different lengths and orientation. Fracture length was assumed to be either uniformly distributed, or following a power law between a minimum and a maximum length. For each scenario the effective hydraulic conductivity was calculated as post-processing. We examined the influence of the following parameters on the conductivity: number of fractures, maximum and minimum fracture length, fracture aperture and the conductivity ratio. Statistics for the results for different parameter settings are presented in boxplots.

For some of the dependencies functional relationships between the parameters of the multi-fracture setting and the resulting mean conductivities are determined. Positive correlations were found between the effective hydraulic conductivity with the number of fractures and with the maximum fracture length. The dependency on maximum fracture length is even better represented by quadratic and cubic functions. The effective conductivity increases with the ratio of hydraulic conductivities.

An accuracy check was performed comparing integrated inflow and outflow values, as utilized in equation (4). Mesh refinement turned out to be crucial, especially for high conductivity ratios. The overall mesh was refined with an additional refinement along the fractures. For the highest conductivity ratios of 10000 and 80 fractures the number of DOFs could reach values above 1.5 Mio. However, the execution time for a single scenario on a standard laptop was seldom longer than 2 minutes.

The results of the simulations and the statistics provide clues how the hydraulic conductivity of a sample is affected by properties of the fracture network. The presented approach may enable the prediction of the effective conductivity of a sample from basic fracture characteristics.

References

1. Berre I., Doster F. Keilegavlen E., Flow in fractured porous media: a review of conceptual models and discretization approaches, *Transport in Porous Media*, **130**, 215-236 (2019)
2. Holzbecher E., Benchmarking model approaches for thin structures in a porous matrix, *The Intern. Journal of Multiphysics*, to appear (2020)
3. Kristinof R., Ranjith P. G, Choi S. K., Finite element simulation of fluid flow in fractured rock media, *Environ Earth Sci*. **60**, 765–773 (2010)
4. Nandlal K., Weijermars R., Impact on drained rock volume (DRV) of storativity and enhanced permeability in naturally fractured reservoirs: upscaled field case from hydraulic fracturing test site (HFTS), Wolfcamp formation, Midland Basin, West Texas, *Energies*, **12**, 3852 (2019)
5. Perko J., Seetharam S., Mallants D., Verification and validation of flow andtransport in cracked saturated porous media, COMSOL Conf., Proceedings, Stuttgart (2011)
6. Radicchi F., Underestimating extreme events in power-law behavior due to machine-dependent cutoffs, *Phys. Rev. E*. **90**, 050801(R) (2014)
7. Romano-Perez C.A., Diaz-Viera M.A., A comparison of discrete fracture models for single phase flow in porous media by COMSOL Multiphysics® software, COMSOL Conf., Proceedings, Boston (2015)
8. Sato K., *Complex Analysis for Practical Engineering*, 309p, Springer, Heidelberg (2015)
9. Schwenck N., Flemisch B., Helmig R., Wohlmuth B.L., Dimensionally reduced flow models in fractured porous media: crossings and boundaries, *Comput. Geosciences*, **19**, 1219–1230 (2015)